

# Transverse single spin asymmetry measurement for very forward neutron production at the RHICf experiment

---

**Minho Kim\*** for the RHICf collaboration

*RIKEN BNL Research Center*

*E-mail:* [mhkim.co.kr@gmail.com](mailto:mhkim.co.kr@gmail.com)

In polarized  $p + p$  collisions, the transverse single spin asymmetry for very forward neutron production was measured by the PHENIX experiment at three different collision energies, 62, 200, and 500 GeV. It has been explained by an interference between  $\pi$  (spin-flip) and  $a_1$  (spin non-flip) exchange with a non-zero phase shift predicting that the asymmetry increases in magnitude with transverse momentum ( $p_T$ ) without longitudinal momentum fraction ( $x_F$ ) dependence. Recently, the asymmetry measured by the PHENIX at 200 GeV was unfolded and showed a good agreement with the model prediction. In June 2017, the RHICf experiment measured the transverse single spin asymmetry for very forward neutron production at  $\sqrt{s} = 510$  GeV up to  $p_T \sim 1$  GeV/c to test a validity of the  $\pi$  and  $a_1$  exchange model in a wide  $p_T$  coverage. In the low  $p_T$  region of  $p_T < 0.25$  GeV/c where the unfolded PHENIX result exists, the neutron asymmetry was consistent with that of PHENIX showing no  $x_F$  dependence. In the high  $x_F$  region of  $x_F > 0.46$ , the asymmetry increases in magnitude with  $p_T$  as the model predicted. However, in the higher  $p_T$  region,  $p_T > 0.25$  GeV/c, there seems a  $x_F$  dependence which has not been expected.

*Presented at DIS2022*

*XXIX International Workshop on Deep-Inelastic Scattering and Related Subjects*

*2-6 May, 2022*

*Santiago de Compostela, Spain*

---

\*Speaker.

## 1. Introduction

Since a large transverse single spin asymmetry ( $A_N$ ) for very forward ( $\eta > 6$ ) neutron production has been discovered by a polarimeter development experiment [1], it has been measured by the PHENIX experiment at three different collision energies, 62, 200, and 500 GeV [2]. One pion exchange (OPE) model which had successfully described the cross section of the neutron production introduced an interference between the spin flip  $\pi$  exchange and spin non-flip  $a_1$  exchange with a relative phase shift to reproduce the experimental data [3]. Though the cross section of the  $a_1$  production is small, it can be replaced by  $\pi\rho$  in the  $1 + S$  state. The  $\pi$  and  $a_1$  exchange model reproduced the data well predicting that the  $A_N$  increases in magnitude with transverse momentum ( $p_T$ ) without longitudinal momentum fraction ( $x_F$ ) dependence. Recently, the neutron  $A_N$  measured by the PHENIX experiment at  $\sqrt{s} = 200$  GeV was unfolded to precisely study the kinematic dependence of the neutron  $A_N$  and showed a consistency with the model prediction [4].

In polarized  $p + p$  collisions, the  $A_N$  is defined by a left-right cross section asymmetry,

$$A_N = \frac{\sigma_L - \sigma_R}{\sigma_L + \sigma_R},$$

where the  $\sigma_{L(R)}$  is the cross section of a particle which is produced in the left (right) side with respect to the beam polarization. While the PHENIX data can test the  $\pi$  and  $a_1$  exchange model only in the low  $p_T$  region, the RHICf experiment [5] measured the neutron  $A_N$  up to the highest  $p_T$  region  $\sim 1$  GeV/ $c$  ever measured to study the validity of the  $\pi$  and  $a_1$  exchange model in a wide  $p_T$  coverage.

## 2. RHICf experiment

In June 2017, The RHICf experiment measured the  $A_N$  for very forward neutron production in polarized  $p + p$  collisions at  $\sqrt{s} = 510$  GeV at the Relativistic Heavy Ion Collider (RHIC).

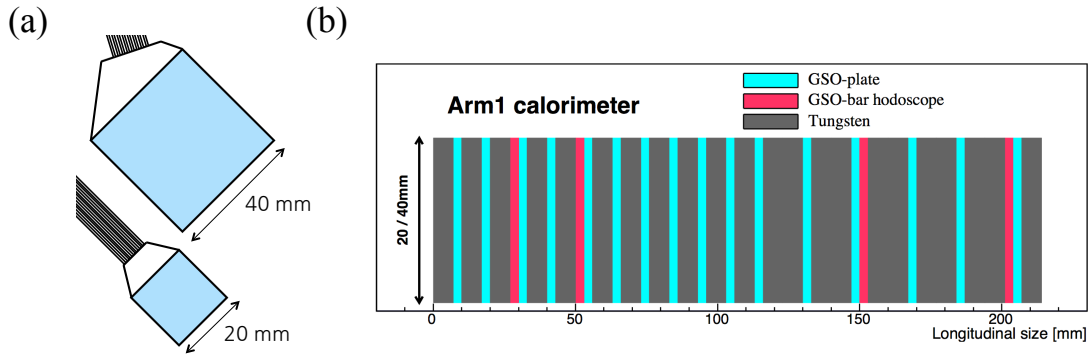


**Figure 1:** Schematic drawing of the (a) front view and the (b) longitudinal structure of the RHICf detector.

An electromagnetic calorimeter (RHICf detector) was installed in front of the STAR Zero-Degree Calorimeter (ZDC) [6], which was located 18 m away from the beam interaction point to measure the very forward neutral particles including the neutron. Figure 1 shows the schematic drawing of

the RHICf detector. As shown in Fig. 1 (a), the RHICf detector consists of small and large sampling towers with 20 and 40 mm dimensions, respectively. They have same longitudinal structure as shown in Fig. 1 (b). They are composed of 17 tungsten absorbers with 1.6 interaction length in total, 16 GSO plates for energy measurement, and 4 layers of GSO bar hodoscope for position measurement. Position and energy resolutions for 250 GeV neutron are about 1 mm and 35% when the incident position of the neutron is the center of a tower. A shower trigger which was operated when the energy deposits of three successive GSO plate layers are larger than 45 MeV was used for the neutron measurement. For more detailed detector configuration and performance, see [7], [8], and [9].

We requested large  $\beta^*$  value of 8 m at operation to make the angular beam divergence small. Corresponding luminosity at  $\sqrt{s} = 510$  GeV was  $\sim 10^{31} \text{ cm}^{-2}\text{s}^{-1}$  which was smaller than that in usual RHIC operation. We also requested a radial polarization which was  $90^\circ$ -rotated from that of usual RHIC operation to reach the maximal  $p_T$  range by moving the detector vertically. We took the data during about 28 hours with three detector positions where the beam headed the center of large tower, center of small tower, and 24 mm below the center of smaller tower.

### 3. Data analysis

The shower trigger is sensitive to not only the neutron events but also the photon events. The neutron events were separated from the photon background using so called  $L_{20\%}$  and  $L_{90\%}$  variables.  $L_{X\%}$  is defined by the longitudinal depth of the detector where the accumulated energy deposit

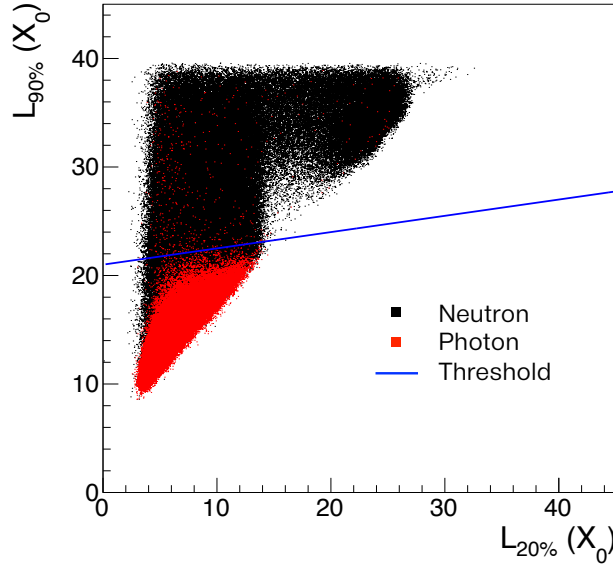


**Figure 2:**  $L_{90\%}$  versus  $L_{20\%}$  distributions of the neutron and photon events generated by QGSJET-II 04 [11]. A particle is considered as a neutron if the  $(L_{20\%}, L_{90\%})$  is located above the blue line.

reaches  $X\%$  of total of the energy deposit. Figure 2 shows the  $L_{90\%}$  versus  $L_{20\%}$  distributions of the

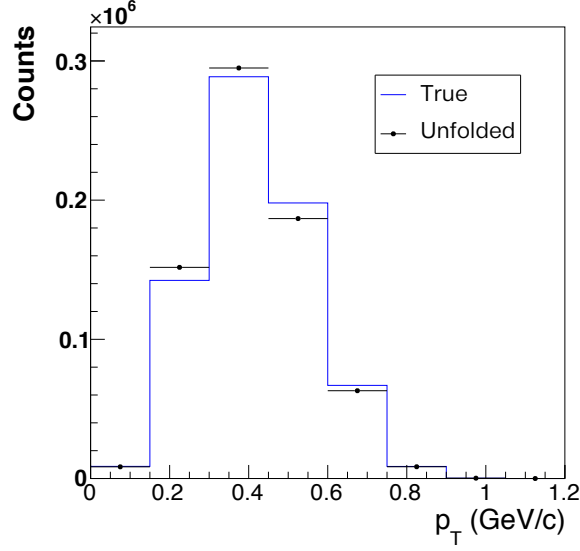


**Figure 3:** True and unfolded  $p_T$  distribution of neutron. Neutron sample generated by the QGSJET-II 04 was used.

neutron and photon events. A particle was considered as neutron if the  $(L_{20\%}, L_{90\%})$  was above a first polynomial which was optimized taking into account the neutron purity and efficiency.

Since the RHICf detector has insufficient interaction length for the neutron energy measurement, reconstructed  $x_F$  and  $p_T$  is quite smeared to the neighboring bins. In order to estimate the kinematic dependence of the neutron  $A_N$  precisely, two-dimensional Bayesian unfolding [12] was applied for  $x_F$  and  $p_T$ . To build a response matrix, single neutrons were generated by randomizing the energy and traveling direction so that they uniformly hit the whole area of the detector. Figure 3 shows the true and unfolded  $p_T$  distribution when the neutron sample from the QGSJET-II 04 was used as an input. Unfolded  $p_T$  versus  $x_F$  distribution was projected to the  $p_T$ -axis to estimate the one-dimensional distribution. One can see the unfolded distribution reproduces the input distribution well.

After unfolding, background  $A_N$ s from the photon and charged hadron were subtracted using the following equation,

$$A_N^{\text{neu}} = \left(\frac{N_{\text{total}}}{N_{\text{neu}}}\right)A_N^{\text{total}} - \left(\frac{N_{\text{pho}}}{N_{\text{neu}}}\right)A_N^{\text{pho}} - \left(\frac{N_{\text{had}}}{N_{\text{neu}}}\right)A_N^{\text{had}},$$

where the notations “neu”, “pho”, and “had” mean the neutron, photon, and charged hadron events, respectively.  $N$  is the number of measured events for each event type. Ratios of each event type to the neutron event,  $N_{\text{total}}/N_{\text{neu}}$ ,  $N_{\text{pho}}/N_{\text{neu}}$ , and  $N_{\text{had}}/N_{\text{neu}}$ , were estimated referring to their spectra in the QGSJET-II 04.  $A_N^{\text{pho}}$  was calculated using the photon-enhanced sample which was selected using the threshold line in Fig. 2. Since the  $A_N^{\text{had}}$  is not quantitatively estimated yet, a large systematic uncertainty was assigned to the  $A_N^{\text{neu}}$  as a difference between when -1 and +1 which were the minimum and maximum  $A_N$  values a particle can have were substituted to the  $A_N^{\text{had}}$ .

#### 4. Results

Figure 4 shows the preliminary result for very forward neutron  $A_N$  as functions of  $p_T$  and  $x_F$ . In Fig. 4 (a), the neutron  $A_N$ s measured by the RHICf experiment are consistent with those of PHENIX [4] in the low  $p_T$  region of  $p_T < 0.25$  GeV/c without showing  $x_F$  dependence. In the two higher  $x_F$  ranges,  $0.46 < x_F < 0.64$  and  $0.64 < x_F < 1.00$ , the  $A_N$  increases in magnitude with  $p_T$

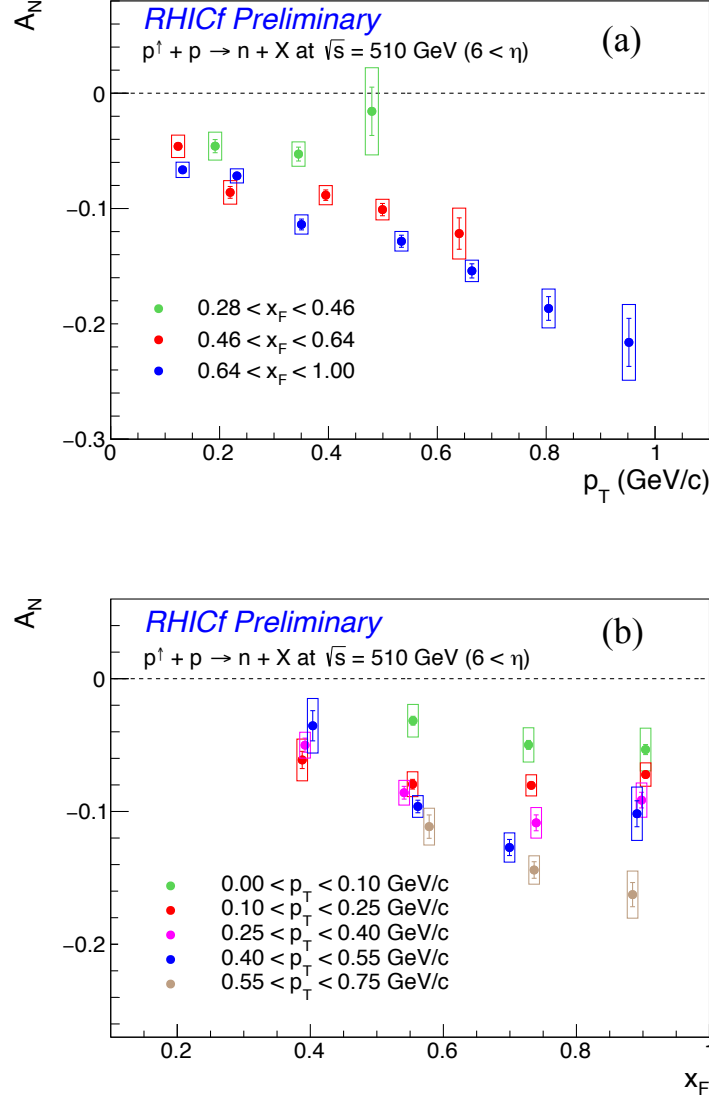


**Figure 4:**  $A_N$  for very forward neutron production (a) as a function of  $p_T$  in three different  $x_F$  ranges and (b) as a function of  $x_F$  in five different  $p_T$  ranges.

as the model predicted. However, it shows a different behavior in the lowest  $x_F$  range. There seems a gap which indicates a possible  $x_F$  dependence between different  $x_F$  ranges.

In Fig. 4 (b), no  $x_F$  dependence is observed in the two lowest  $p_T$  ranges showing flat  $A_N$ s. These are consistent result with those of PHENIX. Though they are flat, the  $A_N$ s in the higher

$p_T$  range are bigger because they increase following the  $p_T$ . However, a clear  $x_F$  dependence is observed in the other higher  $p_T$  ranges which has been not expected by the  $\pi$  and  $a_1$  exchange model.

## 5. Summary

In June 2017, the RHICf experiment measured the  $A_N$  for very forward neutron in polarized  $p + p$  collisions at  $\sqrt{s} = 510$  GeV to test the  $\pi$  and  $a_1$  exchange model in a wide  $p_T$  coverage up to about 1 GeV/ $c$ . In the higher  $x_F$  region of  $x_F > 0.46$ , the neutron  $A_N$  increases in magnitude with  $p_T$  as the model predicted. In the lower  $p_T$  region of  $p_T < 0.25$  GeV/ $c$ , the  $A_N$ s are consistent with the recently unfolded PHENIX result showing no  $x_F$  dependence. However, in the other higher  $p_T$  region, though a large systematic uncertainty was assigned to the background  $A_N$  subtraction procedure, a  $x_F$  dependence was observed. With more precise background estimation, the neutron  $A_N$  analysis at RHICf will be finalized soon.

**Acknowledgements** This program is partly supported by the U.S.-Japan Science and Technology Cooperation Program in High Energy Physics, JSPS KAKENHI (No. JP26247037 and No. JP18H01227), the joint research program of the Institute for Cosmic Ray Research (ICRR), University of Tokyo, and the National Research Foundation of Korea (No. 2018R1A5A1025563), and “UNICT 2020-22 Linea 2” program, University of Catania.

## References

- [1] Y. Fukao *et al.*, Phys. Lett. B **650**, 325 (2007).
- [2] K. Tanida (PHENIX Collaboration), J. Phys. Conf. Ser. **295**, 012097 (2011).
- [3] B. Z. Kopeliovich, I. K. Potashnikova, I. Schmidt, and J. Soffer, Phys. Rev. D **84**, 114012 (2011).
- [4] U. A. Acharya *et al.* (PHENIX Collaboration), Phys. Rev. D **103**, 052009 (2021).
- [5] RHICf Collaboration: LOI, arXiv: 1409.4860v1.
- [6] C. Adler *et al.*, Nucl. Instrum. Meth. A **470**, 488 (2001).
- [7] T. Suzuki *et al.*, JINST **8**, T01007 (2013).
- [8] Y. Makino *et al.*, JINST **12**, P03023 (2017).
- [9] K. Kawade *et al.*, JINST **9**, P03016 (2014).
- [10] M. H. Kim *et al.* (RHICf Collaboration), Phys. Rev. Lett. **124**, 252501 (2020).
- [11] S. Ostapcheno, Nucl. Phys. B, Proc. Suppl. **151**, 143 (2006).
- [12] G. D’Agostini, Nucl. Instrum. Meth. A **362**, 487 (1995).